Indian Journal of Advances in Chemical Science

Article

Synthesis of Hybrid Cassava Starch Composite and its Application for Methylene Blue Adsorption

N'guadi Blaise Allou[1]*, N'goran Sévérin Eroi[2], Mougo André Tigori[3], Bangaly Kaba[1], Aphouet Aurélie Koffi[1], Patrick Atheba[1], Albert Trokourey[1]

[1]Laboratoire de Constitution et Réaction de la Matière, UFR SSMT, Université Félix Houphouët Boigny, Abidjan, Côte d'Ivoire, [2]Laboratoire de Thermodynamique et de Physico–Chimie du Milieu, UFR SFA, Université Nangui Abrogoua, Abidjan, Côte d'Ivoire, [3]Laboratoire des Sciences et Technologies de l'Environnement, UFR Environnement, Université Jean Lorougnon Guédé, Daloa, Côte d'Ivoire

ABSTRACT

One of the major problems of sub-Saharan Africa is the non-treatment of industrial effluents which are directly discharged into the environment. It is therefore crucial to develop inexpensive adsorbents to overcome these problems by treating water by adsorption. This study focuses on the development of low-cost hybrid composite based on cassava starch for the removal of methylene blue from aqueous medium. Thus, carbon particles from popcorn were deposited on the surface of cassava starch which had previously undergone destructuring by acid hydrolysis. The prepared adsorbent was characterized by X-ray diffraction and scanning electron spectroscopy. The effectiveness of the hybrid composite was verified by varying parameters such as contact time, adsorbent dose, pH, temperature, and initial pollutant concentration. Analysis of isotherm model that can describe the adsorption phenomenon indicated that the experimental data fit Langmuir model better with correlation coefficients approaching unity and separation factor values (R_L) indicating a favorable process. The maximum monolayer adsorption capacity was 6.44 mg/g. Adsorption kinetic results were better explained by pseudo–second-order model. The spontaneous and exothermic character of the adsorption process was revealed by thermodynamic study. Hybrid composite reuse was evaluated and excellent results were obtained. Therefore, hybrid composite based on cassava starch and carbons derived from popcorn is a cheap adsorbent for the removal of methylene blue from aqueous solutions.

Key words: Cassava starch, Popcorn, Activated carbon, Composite, Methylene blue, Adsorption.

1. INTRODUCTION

In recent decades, the development of human industrial activities has generated a wide variety of chemical products which, without treatment and carelessness, are discharged into the water cycle. These substances contained in wastewater are difficult to biodegrade and their accumulation in waterways causes problems to environment and public health [1]. It is therefore necessary to identify these harmful substances and find effective treatment methods.

Most of the time, discharges of contaminated effluents come from chemical, petrochemical, agro-food, textile, paper mill, tanneries industries, and particularly beverage industries, which are much more toxic, because contain huge amounts of organic matter [2,3]. One of the major pollutants from these industrial discharges remains dyes. Once dissolved in water, dyes are sometimes difficult to process because they are often of synthetic origin and have a complex molecular structure which makes them more stable and difficult to biodegrade [4,5]. Most dyes are toxic, carcinogenic, cause allergies, and irritate the skin [6-8]. Thus, they constitute risk factors for human and aquatic health, and nuisance for environment.

Many techniques were proven in the removal of dyes from wastewater, including traditional physicochemical methods, biological methods and advanced oxidation treatments [9,10], ozonation [11,12], photocatalysis [13,14], and absorption [15-17]. However, adsorption remains, with respect to other methods, the most effective and inexpensive technique. Adsorption is a fundamental process in the physicochemical treatment of effluents which are suitable economically to the reuse of wastewater.

For more than 20 years, the development of hybrid materials has aroused great interest, both in the academic and industrial worlds. Combining the properties of certain organic compounds and those of mineral compounds in a single material has therefore become an achievable objective. Among the different possible strategies for developing hybrid materials, the one that consists of associating calibrated nano-objects (nanoparticles) with a polymer component has many advantages. Recently, several afford were paid to improve adsorbents efficiency and stability for wastewater treatment by the combination of polymers and modified carbon particles [18-20]. The adsorbents resulting from these works showed improved adsorption properties when applied to remove different pollutants.

***Corresponding author:**
N'guadi Blaise Allou
Email: goswamirl@neist.res.in

ISSN NO: 2320-0898 (p); 2320-0928 (e)
DOI:10.22607/IJACS.2023.1103004

Received: 25th June 2023;
Revised: 26th July 2023;
Accepted: 27st July 2023

In view of all the above, the main objective of this project is to synthesize a hybrid adsorbent to remove a dye contained in an aqueous solution. To achieve this objective, a nanocomposite based on cassava starch and carbon nanoparticles derived from popcorn will be synthesized. The efficiency of the nanocomposite obtained will be highlighted by adsorption of methylene blue through all the parameters that can influence an adsorption process to determine the optimal adsorption conditions. The interest in the design of such a nanocomposite lies in the use of low-cost and biorenewable materials.

2. MATERIALS AND METHODS

2.1. Materials

Corn grains as well as the starch used as biomass during this work were purchased on the local market. Potassium hydroxide (KOH), sodium hydroxide (NaOH), hydrochloric acid (HCl), citric acid ($C_6H_8O_7$), and methylene blue ($C_{16}H_{18}ClN_3S$) were the chemicals used in this study. Figure 1 presents the molecular structure of methylene blue (MB) and Table 1 its physicochemical properties. All chemicals were used as received without any purification. Water used to prepare the solutions is distilled water.

2.2. Carbon Particles Derived from Popcorns Preparation

Popcorns were obtained using cooking pots. In practice, 200 g of corn kernels were enclosed in a pot and heated for 7 min. Then, on that date, water inside the hot grains was vaporized and the starch liquefied, forming popcorns. After that, the popcorns were crushed using a blender and made into powder through porcelain mortar. The white powder obtained was carbonized at 400°C for 1 h under an inert atmosphere with a heating rate of 5°C/min to obtain a black powder. Then, 10 g of the obtained black powder and 200 ml of 1M KOH solution were shaken during 5 h followed by the filtration of the resulting mixture and dried in oven. The resulting black solid was later crushed and transferred to a furnace for activation at 800°C for 1 h under a nitrogen atmosphere. Finally, the prepared activated carbon (AC) was washed with HCl (1M) to remove inorganic impurities, then with distilled water until the water in the filtrate became neutral and dried in oven at 110°C for 48 h.

2.3. Carbon@starch (C@St) *Composite Preparation*

The preparation of C@St composite was carried out according to the work described by Allou *et al.* [21] with minor modifications. Starch grains underwent structural and functional modification by arranged acid hydrolysis to improve their performance. Thus, 100 ml of 0.25 mol/L hydrochloric acid and 20 g of cassava starch were introduced into 250 ml conical flask. The whole was subjected to magnetic stirring for 30 min and at 100°C. The modified starch obtained was filtered, dried in oven for 48 h, and named St in the context of this study.

Regarding the preparation of C@St composite, a reactor containing 10 g of modified cassava starch, 1 g of AC from popcorn, and 500 ml of distilled water was shaken at room temperature for 24 h. Then, citric acid (powder) was added to the polymer solution so that its final concentration was approximately 1 g/L. The solution was homogenized by vigorous stirring for 2 h. The homogeneous solution obtained was transferred to a glass container and dried in oven during 24 h to evaporate water. The curing step was finally done by heating the polymer composite at 80°C during 24 h.

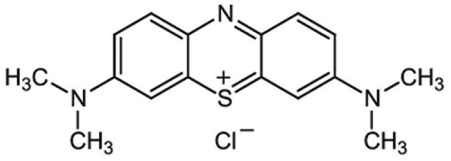

Figure 1: Methylene blue molecular structure.

Table 1: Methylene blue physicochemical properties.

Parameter	Value
Molecular formula	$C_{16}H_{18}ClN_3S$
Molecular weight ($g.mol^{-1}$)	319.85
Dye family	Basic
Water solubility at 20°C ($g.L^{-1}$)	20
Maximum wavelength (nm)	665

2.4. Material Characterization Methods

To ensure the success of the adsorbents preparation, certain characterizations are necessary. Therefore, samples of the materials were subjected to analyze such as X-ray diffraction (XRD) and scanning electron microscopy (SEM).

The crystalline structure of the different synthesized materials was determined using a Rigaku Ultima IV model Advance type diffractometer using monochromatic copper Kα radiation (CuKα radiation) (λ = 1.54 Å) at voltage of 40 kV and current of 40 mA. The measurements were carried out on non-oriented samples in powder form with particle size less than or equal to 100 µm in the range of the Bragg angle ranging from 3° to 70° with a pitch of 0.02 and counting time 10.1 seconds per step.

Carl Zeiss type scanning electron microscope (Sigma VP) was used to observe the particles morphology of the synthesized materials. Before observation, a small quantity of the material powder was deposited, using a spatula, on a double-sided carbon sticker and the excess particles were removed from atomized air.

2.5. Batch Adsorption Experiments

Adsorption properties, in discontinuous mode, of C@St composite were evaluated using 50 ml of methylene blue (MB) as pollutant in 250 ml Erlenmeyer flasks. As is customary in adsorption study, the influence of equilibrium time, adsorbent dose, initial solution pH, initial dye solution concentration, and temperature, in different slices, were evaluated. The desired pH was obtained by adding few drops of 0.1N HCl or NaOH. The residual MB concentration was calculated by measuring the absorbance using UV-visible spectrophotometer at a wavelength of 662 nm.

The percentage of BM adsorbed as well as the adsorption capacity q_e (mg/g) at equilibrium were calculated according to equations (1) and (2) [22] in which C_i (mg/L) and C_e (mg/L) are the initial and equilibrium concentrations of MB, respectively, V (L) and W (g) are the volume of the solution and the mass of the adsorbent, respectively.

$$\%\ BM\ adsorbé = \frac{C_i - C_e}{C_i} \times 100 \quad (1)$$

$$q_e = \frac{C_i - C_e}{W} \times V \quad (2)$$

To be reused, after adsorption on 0.2 g of the adsorbent in 50 ml of 5 mg/L MB solution, the adsorbent is removed and washed with 0.1N HCl and distilled water under constant stirring 3 times, respectively, then dried at 80°C for 24 h. The recycled adsorbent is again added to another MB solution to start a new adsorption.

2.6. Adsorption Kinetic and Isotherm Models

Adsorption kinetics is one of the parameters indicating the purification performance of an adsorbent. Adsorption kinetics of the material can be modeled. To this end, the literature reports a number of models such as pseudo–first-order model, pseudo–second-order model, intraparticle diffusion model and Elovich model. As for the adsorption isotherm models, those commonly used are Langmuir, Freundlich, and Temkin models. Table 2 presents the linear equations, the plotted curves, as well as the calculated parameters for both kinetic and isotherm models. However, one of the most important Langmuir parameters, namely, separation factor (R_L), indicating the favorability of the adsorption process, can be calculated using equation (3).

$$R_L = 1/(1+k_L C_0) \quad (3)$$

3. RESULTS AND DISCUSSION

3.1. Adsorbent Characterization

The crystalline character of activated carbon derived from popcorn, modified starch, and C@St composite was determined by XRD analysis and patterns obtained are shown in Figure 2. AC pattern shows broad peak centered at around 26°, relative to (002) plane of AC particles, suggesting the amorphous character of the prepared carbon. The pattern of St and C@St samples reveal peaks at 15.23° and 23.08°

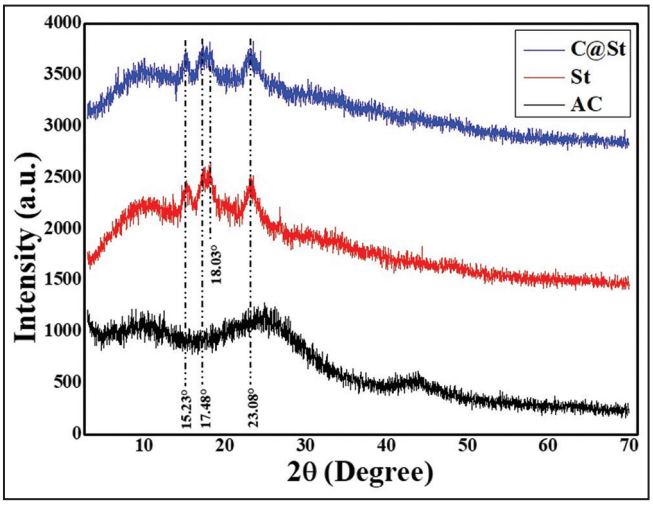

Figure 2: X-ray diffraction patterns of popcorn-derived activated carbon, modified starch (St), and composite carbon@starch.

and a doublet at 17.48° and 18.03° particularly for St. These peaks are typical of cereal-derived starches [30,31]. However, the incorporation of AC into the starch decreases the intensity of the peaks indicating a decrease of the crystallinity of starch.

Figure 3 shows a microscopic image of AC as well as that of C@St composite. A rough surface with pores in places is observed for the AC. As for the micrograph of the composite, a predominant spherical granulometry is observed [31] with black spots on the surface of the spheres. These black dots could be due to the presence of carbon particles.

3.2. Methylene Blue Adsorption Conditions Study

3.2.1. Adsorbent dose effect

The quantity of adsorbent used constitutes one of the most determining parameters in the process of mass transfer during adsorption. Indeed, this quantity guarantees the presence of a sufficient number of active sites to interact with the molecules or ions in solution. Figure 4 illustrates the relationship between adsorbent dose used and MB percentage eliminated for a concentrated solution at 25 mg/L. It appears from this figure that the greater the mass of the adsorbent, the greater the quantity of MB eliminated. This observation would be explained by the abundance of the number of free adsorption sites by increasing the mass. However, from a mass of 0.15 g, the percentage of MB adsorbed remains almost unchanged due to the depletion of MB cations in the solution. Hence, using a mass beyond, this limit would amount to making an unnecessary expenditure in mass. Therefore, for the rest of the work, the optimal mass of 0.15 g for 50 ml, that is, 3 g/L was used.

3.2.2. Effects of contact time and initial solution concentration

The study of initial dye concentration and contact time effects of MB adsorption on C@St was carried out and the results are shown in Figure 5. The curves obtained show striking similarities, being divided into two distinct parts. The first part, almost vertical, reflects a rapid fixation of large quantities of dye, while the second part, horizontal, represents a plateau of equilibrium. The immediate availability of free adsorption sites on the adsorbent surface from the first contact would explain the extremely rapid MB adsorption process during the 1st min. However, as the number of free sites decreases, the adsorption gradually slows down to equilibrium, indicating the occupation of almost all free adsorption sites. Furthermore, it should be noted that the lower the initial concentration of the solution (7 and 20 mg/L), the faster equilibrium is reached (around 10 and 30 min). This observation could be attributed to the wide availability of free adsorption sites for a small

Table 2: Kinetic and isotherm adsorption models used to analyze MB adsorption*.

Model	Equation	Plot	Parameter	References
Pseudo–first-order	$\ln(q_e - q_t) = \ln q_e - k_1 t$	$\ln(q_e - q_t)$ versus t	k_1, $q_{e,cal}$	[23]
Pseudo–second-order	$t/q_t = 1/k_2 q_e^2 + t/q_e$	t/q_1 versus t	k_2, $q_{e,cal}$	[24]
Intraparticle diffusion	$q_t = k_{id} t^{1/2} + C$	q_1.versus $t^{1/2}$	K_{id}, C	[25]
Elovich	$q_t = In(\alpha\beta)/\beta + \ln t/\beta$	q_t versus Int	α, β	[26]
Langmuir	$1/q_e = 1/q_m + 1/(q_m C_e k_L)$	$1/q_e$ versus $1/C_e$	q_m, k_L, R_L	[27]
Freundlich		versus $In\ C_e$	k_F, n	[28]
Temkin	$qe = B\ In\ A + B\ In\ Ce$	q_e.versus $In\ C_e$	$A.$, $B.$	[29]

*q_e and q_t=Adsorption ca.at equilibrium and at time t, respectively; k_1 and k_2=Rate constant of pseudo–first-order and pseudo–second-order, respectively; α=Initial adsorption rate, β=Exten.su.face coverage, k_{id}=Intraparticle diffusion rate, C=Constant indicating bounda lakness; C_e (mg/L)=adsorbate equilibrium concentration; k_L. (L/mg)=Langmuir constant; (mg/g)=Maximum monolayer adsorption capacity; n and k_F (mg/g)=Freundlich constants related to adsorption and intensity of adsorption driving force or surface heterogeneity, respectively; A=Temkin constants (L/g); B=Constant related to the heat of adsorption and it idefined by the expression $B=RT/b$, b=Temkin constant (J/mol), T=Absolute temperature (K), R=Gas constant (8.314 J/mol.K)

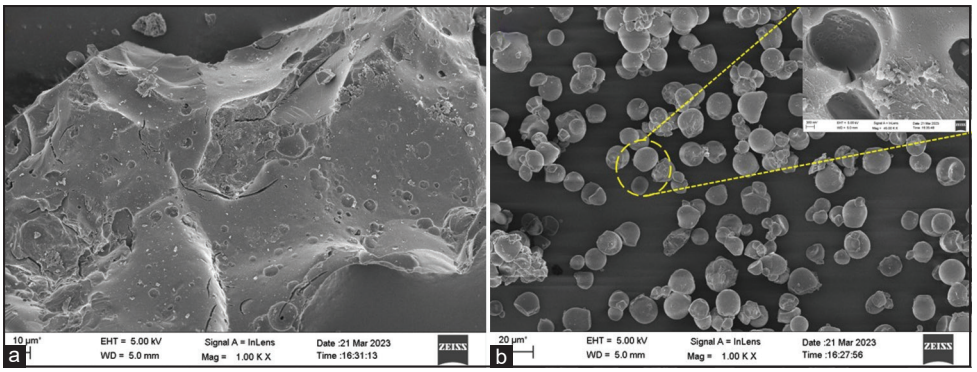

Figure 3: Scanning electron microscopy image of AC (a) and C@St (b).

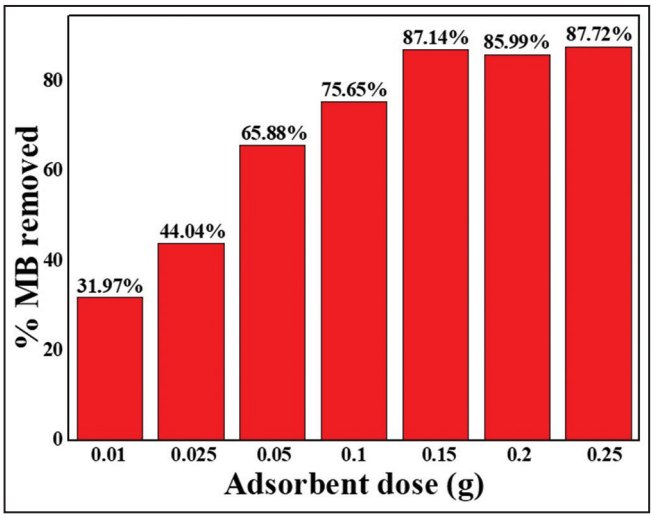

Figure 4: Effect of adsorbent dose on MB removal by C@St.

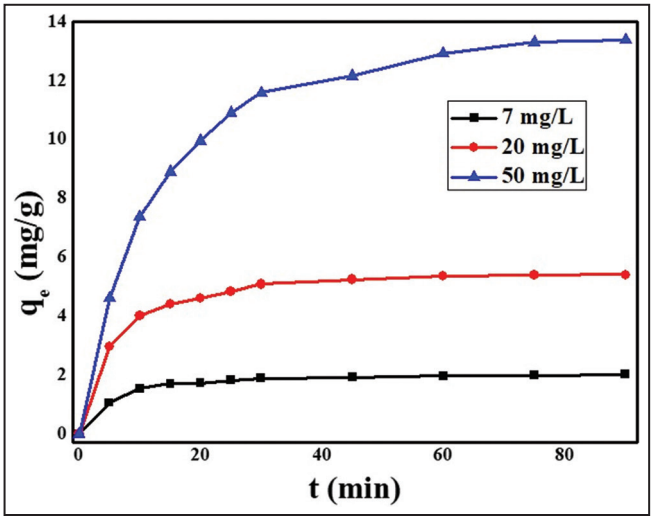

Figure 5: Effect of contact time of MB adsorption on C@St at MB different concentrations.

amount of pollutants [32]. Whereas, for a relatively high concentration (50 mg/L), a long equilibrium time of 90 min is necessary. In addition, it is also noticed that as the initial concentration of pollutant increases the adsorption capacity also increases.

3.2.3. Effect of initial solution pH

The transformation of the surface charge of an adsorbent as well as the degree of ionization of dye molecules are most controlled by the pH

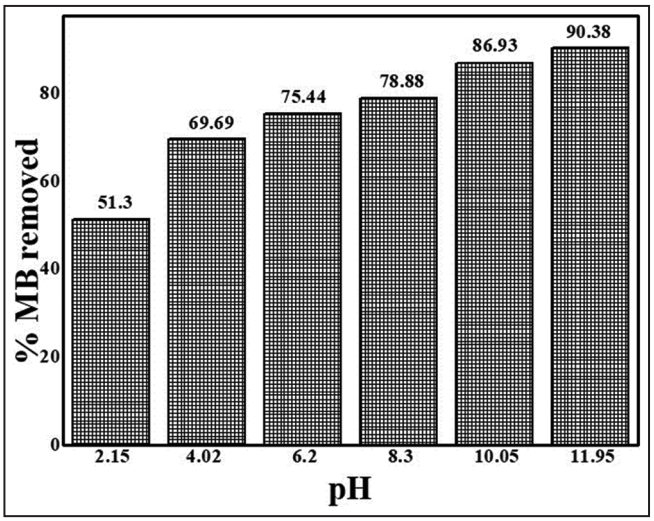

Figure 6: Effect of initial solution pH during the adsorption of MB on C@St.

of the aqueous solution. The impact of the pH of the reaction medium on MB sorption on C C@St was studied and the results presented in Figure 6. The latter indicates that increase in MB percentage eliminated increases with solution pH. Since MB is cationic in aqueous medium, its weak adsorption in acid medium would be explained by the probable competition for binding on the free sites between MB cations and H_3O^+. ions in the medium [33]. Moreover, in basic medium, there is a negative charge on C@St surface, leading to an improvement in the electrostatic interactions between active sites and MB ions, hence a large quantity of MB eliminated.

3.2.4. Adsorption isotherm modeling

The adsorption isotherm is a curve which represents the relation between adsorbate concentration at equilibrium and quantity of adsorbent necessary to reach this state of equilibrium, at a given temperature. The experimental data obtained were subjected to Langmuir, Freundlich, and Temkin models for a deep understanding of the mechanism of MB adsorption on C@St. According to the results presented in Figure 7 and Table 3, Langmuir model, with correlation coefficients of the order of 0.94–0.98 at different temperatures, is best suited to describe the adsorption phenomenon of MB on C@St. Moreover, the calculated R_L.values ($0 < R_L < 1$) indicate a favorable process. This, therefore, suggests that the binding of MB occurs in monolayer on energetically homogeneous adsorption sites and without interaction between the adsorbed dye cations [34]. This model also assumes that saturation of the adsorbent surface is reached when all active sites are occupied by adsorbate molecules, limiting adsorbent maximum adsorption capacity.

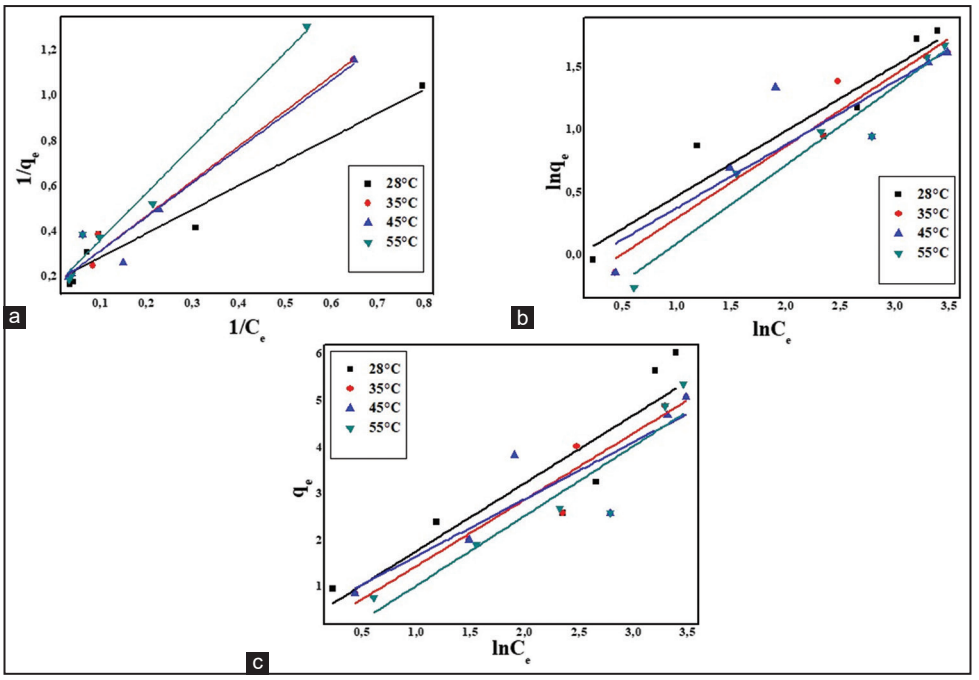

Figure 7: Representation of the adsorption patterns of (a) Langmuir, (b) Freundlich, and (c) Temkin during the adsorption of MB on C@St.

Table 3: Langmuir, Freundlich, and Temkin isotherms parameters of MB adsorption on C@St.

Adsorption isotherm model	Parameter	Temperature (°C)			
		28	35	45	55
Langmuir	$q_{max,\ cal.}$ (mg/g)	5.60	6.24	6,14	6,44
	k_L. (L/mg)	0.168	0.104	0.138	0.075
	R_L	0.125–0.590	0.188–0.700	0.149–0.637	0.243–0.764
	R^2	0.949	0.988	0.949	0.979
Freundlich	k_F ($mg^{1-1/n/n}\ g^{-1}$)	949	0.753	0,877	0,584
	n	1.910	1.732	1.970	1,590
	R^2	913	0.950	0.806	0.946
Temkin	A	1.236	1,.017	1.428	0.730
		1.463	1.428	1.223	1.502
	R^2	0.824	0.935	0.778	0.867

The adsorption efficiency o.he prepared C@St compared to certain values obtained in literature was established in Table 4 by comparing the adsorption capacities. The high adsorption capacity raises the potential of C@St to remove MB ions from an aqueous solution.

3.2.5. Temperature effect and calculation of thermodynamic parameters

Study of the temperature effect on the MB adsorption showed that the adsorption capacity increased slightly when the temperature of the reaction medium increased (Table 2). This would be explained by the fact that the physical interaction between MB and C@St is weakened due to the decrease in hydrogen bonding and Van der Waals interactions [38].

Thermodynamic study gives information on the energy variations as well as the spontaneity or not of the adsorption process. Free energy change (ΔG^o), enthalpy change (ΔH^o), and entropy change (ΔS^o) are calculated using Gibbs–Helmholtz and Van't Hoff relations [22]:

$$\Delta G^o = \Delta H^o - T\Delta S^o \ . \quad (4)$$

Table 4: Comparison of L. ngmuir MB adsorption capacities of different adsorbents.

Adsorbent	Adsorption capacity (mg/g)	References
AC derived from corn cobs	0.84	[35]
AC derived from fir wood	1.21	[36]
	2.51	[34]
Fe_3O_4/AC/cyclodextrin/ sodium alginate	2.079	[33]
Polyacrylonitrile beads grafted with alginate	3.51	[37]
Carbon@starch	6.44	This study

AC: Activated carbon

$$\Delta G^o = -RT\ ln\ k_C \ . \quad (5)$$

In these equations, R is the ide gas constant, k_C (dimensionless) is the equilibrium constant between two phases and *The* absolute temperature.

The isotherm model best decreasing the adsorption phenomenon being that of Langmuir, then k_C corresponds to Langmu eqlibrium constant k_L. (L.mg^{-1}) at each temperature multiplied by the density of water (10^6 mg.L^{-1}). The graphical representation of *In* k_C as a function of $1/T$ used to deterne the thermodynamic parameters is given in Figure 8. These parameters are recorded in Table 5. The negative values of ΔG^o and ΔH^o indicate that the adsorption of MB on C@St controlled by a spontaneous and exothermic process. This behavior seems to be explained by the ionic nature of the MB–C@St interaction. The negative value of ΔS^o indicates that the disorder decreases (randomness) at the solid-solution interface during dye adsorption on the adsorbent [39].

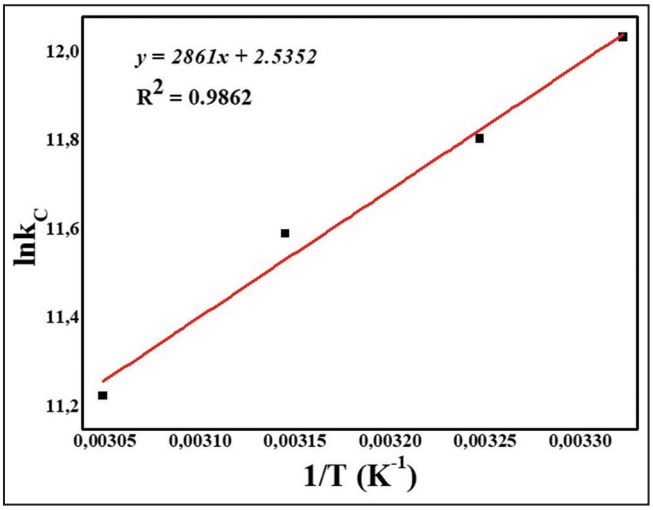

Figure 8: Representation of *In* k_C as a function of $1/T$ for estimating thermodynamic parameters.

3.2.6. Adsorption kinetic modeling

Pseudo–first-order, pseudo–second-order, intraparticle diffusion, and Temkin models were used to describe MB adsorption kinetic on C@St surfaces. The application of the experimental adsorption data to these models is shown in Figure 9 and the various calculated parameters are recorded in Table 6. Based on the correlation coefficients, the pseudo–second-order model is the one that best describes the process of MB adsorption on C@St. This observation would suggest that the overall rate of MB adsorption is controlled by a chemical process through electron sharing or by covalent forces through electrons exchange between adsorbent and adsorbate [40]. Moreover, $q_{e,cal}$ values calculated for MB different initial concentrations are much closer to those measured experimentally, thus confirming the adaptation of this model. Furthermore, the amount of dye adsorbed at equilibrium increases with the initial dye concentration, suggesting an increase in driving force for mass transfer and an increase in the adsorbent surface area covered by dye molecules.

3.2.7. C@St reuse study

Reusability of adsorbent prodes several benefits in the use of adsorption as wastewater treatment method. The most important benefit in the reuse of adsorbent remains the economic value. The results of C@St reusability tests are shown in Figure 10. From the first adsorption test, MB percentage removal decreases slightly from 85.2 % to 66.3% at the

Table 5: Thermodynamic parameters of MB adsorption on C@St.

T (°C)	ΔG^o (J mol^{-1})	H^o (kJ mol^{-1})	S^o (kJ mol^{-1} K^{-1})
28	−30.11		
35	−30.23	−23.79	0.021
45	−30.64		
55	−30.61		

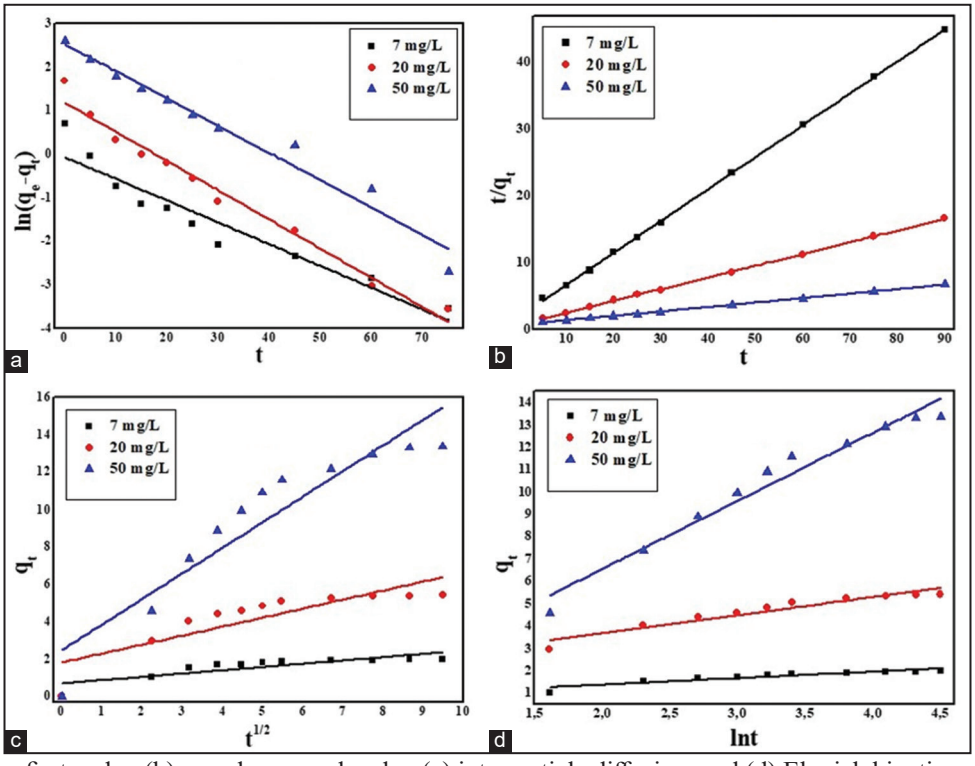

Figure 9: (a) Pseudo–first-order, (b) pseudo–second-order, (c) intraparticle diffusion, and (d) Elovich kinetic models representation during MB adsorption on C@St.

Table 6: Kinetic parameters of MB adsorption on C@St.

C_i (mg/L)	$q_{e,\,exp}$ (mg/g)	Pseudo–first-order			Pseudo–second-order		
		$q_{e,\,exp}$ (mg/g)	k_1 (min^{-1})	R^2	$q_{e,\,exp}$ (mg/g)	k_2 (g/mg/min)	R^2
7	2.01	0.94	–0.0500	0.9124	2.09	0.1205	0.9997
20	5.41	3.28	–0.0672	0.9787	5.70	0.0408	0.9998
50	14.38	12.59	–0.0627	0.9662	15.04	0.0065	0.9993
C_i (mg/L)		Intraparticle diffusion			Elovich		
		k_{di} (mg/g $min^{-1/2}$)	C (mg/g)	R^2	α (mg/g/min)	β (g/mg)	R^2
7		0.0892	0.7530	0.7096	0.646	3.444	0.8691
20		0.4818	1.8118	0.7345	6.420	1.241	0.9217
50		1.3699	2.4842	0.8778	4.916	0.328	0.9659

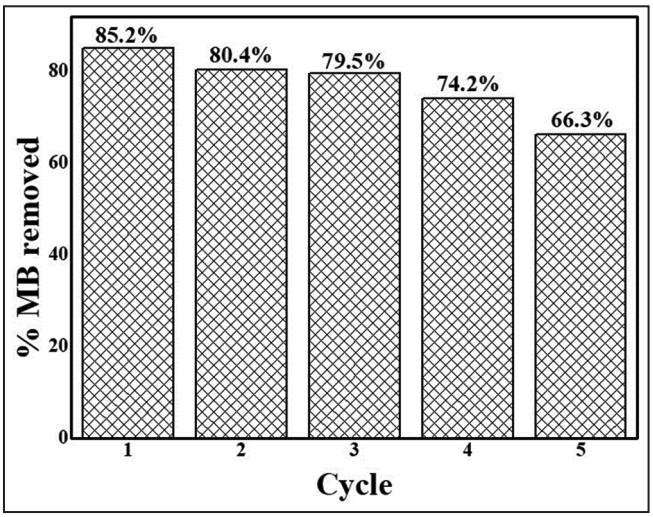

Figure 10: C@St Reuse using 0.1N HCl solution for regeneration up to five MB removal cycles.

fifth adsorption test. It can be assume that even after the fifth cycle of use, the adsorption percentage is much appreciable.

4. CONCLUSION

The present study aimed to prepare a hybrid composite based on cassava starch and carbon particles from popcorn and then test its adsorption properties using methylene blue as pollutant. XRD indicated the amorphous character of the composite while the black spots on the starch spheres surface showed the presence of carbon particles according to the SEM analysis. Several adsorption tests were carried out taking into account certain operational parameters to evaluate the performance of this material.

It appears from these different adsorption tests that a contact time of 90 min, an optimal mass of 3 g/L, and a basic medium are necessary to obtain a better percentage of methylene blue elimination. Langmuir isotherm model was found to be the best model to describe MB adsorption on C@St with a maximum capacity of 6.44 mg/g while the pseudo–second-order kinetic model better explained the kinetic data reflecting a process of chemical adsorption. The adsorption process was rapid at the outer surface of the adsorbent and subsequently followed by a gradual diffusion inside the pores. Thermodynamics showed that the adsorption of MB on C@St was spontaneous and exothermic with a decrease in disorder at the adsorbent–adsorbate interface. In addition, the adsorbent can be reused up to five cycles after regeneration of the latter with a solution of sulfuric acid after each adsorption cycle.

In view of the results obtained, the hybrid composite of cassava starch and popcorn-derived carbon appears as a cheap potential candidate for the removal of methylene blue from aqueous solutions. However, further studies should be carried out to optimize the proportions of each material in the composite. In addition, adsorption tests on real solutions containing other types of organic cations should be carried out.

5. ACKNOWLEDGMENTS

N.B. Allou expresses his gratitude to Dr. Biswajit Saha, Scientist and Lecturer at CSIR–North East Institute of Science and Technilogy, Jorhat, Assam, India, for sample characterizations.

6. STATEMENTS AND DECLARATIONS

6.1. Funding

No fund received from any organization or society.

6.2. Conflicts of Interest

The authors declare that they have no known competing financial interests or personal relationships that could have appeared to influence the work reported in this paper.

7. REFERENCES

1. N. J. Falizi, M. C. Hacifazlioğlu, İ. Parlar, N. Kabay, T. Ö. Pek, M. Yüksel, (2018) Evaluation of MBR treated industrial wastewater quality before and after desalination by NF and RO processes for agricultural reuse, ***Journal of Water Process Engineering***, **22:** 103-108.
2. M. D. Andere, E. Abuto, (2021) Determination of selected heavy metals from treated industrial waste discharge in tea industries and sugar industries, ***Medical and Analytical Chemistry International Journal***, **5:** 000173.
3. A. Rai, P. S. Chauhan, S. Bhattacharya, (2018) Remediation of industrial effluents. In: ***Water Remediation, Energy, Environment, and Sustainability***, Singapore: Springer, p171-187.
4. R. Jamee, R. Siddique, (2019) Biodegradation of synthetic dyes of textile effluent by microorganisms: An environmentally and economically sustainable approach, ***European Journal of Microbiology and Immunology (Bp)***, **9:** 114-118.
5. N. Al-Khatib, J. A. H. Shoqeir, G. Özerol, L. Majaj, (2017) Governing the reuse of treated wastewater in irrigation: The case study of Jericho, Palestine, ***International Journal of Global Environmental Issues***, **16:** 135-148.
6. K. T. Chung, (2016) Azo dyes and human health: A review, ***Journal***

of Environmental Science and Health, Part C Environmental Carcinogenesis Reviews, **34:** 233-261.
7. L. He, F. Michailidou, H. L. Gahlon, W. Zeng, (2022) Hair dye ingredients and potential health risks from exposure to hair dyeing, ***Chemical Research in Toxicology***, **35:** 901-915.
8. C. Symanzik, K. Koopmann, C. Skudlik, S. M. John, W. Uter, **(2023)** Bleaching powders, bleaching creams and other hair lightening preparations as sources for (airborne) allergic contact dermatitis and other health effects in hairdressers: Results of an empirical study, ***Contact Dermatitis***, **88:** 139-144.
9. L. Liu, Z. Chen, J. Zhang, D. Shan, Y. Wu, L. Bai, B. Wang, (2021) Treatment of industrial dye wastewater and pharmaceutical residue wastewater by advanced oxidation processes and its combination with nanocatalysts: A review, ***Journal of Water Process Engineering***, **42:** 102122.
10. G. A. Ismail, H. Sakai, (2022) Review on effect of different type of dyes on advanced oxidation processes (AOPs) for textile color removal, ***Chemosphere***, **291:** 132906.
11. A. R. Tehrani-Bagha, N. M. Mahmoodi, F. M. Menger, (2010) Degradation of a persistent organic dye from colored textile wastewater by ozonation, ***Desalination***, **260:** 34-38.
12. U. Y. Qazi, R. Iftikhar, A. Ikhlaq, R. Jaleel, R. Nusrat, R. Javaid, (2022) Application of Fe-RGO for the removal of dyes by catalytic ozonation process, ***Environmental Science and Pollution Research International***, **29:** 89485-89497.
13. M. Ahmaruzzaman, S. R. Mishra, (2021) Photocatalytic performance of g-C_3N_4 based nanocomposites for effective degradation/removal of dyes from water and wastewater, ***Materials Research Bulletin***, **143:** 111417.
14. M. Hasanpour, M. Hatami, (2020) Photocatalytic performance of aerogels for organic dyes removal from wastewaters: Review study, ***Journal of Molecular Liquids***, **309:** 113094.
15. O. A. Shabaan, H. S. Jahin, G. G. Mohamed, (2020) Removal of anionic and cationic dyes from wastewater by adsorption using multiwall carbon nanotubes, ***Arabian Journal of Chemistry***, **13:** 4797-4810.
16. A. Gil, F. C. C. Assis, S. Albeniz, S. A. Korili, (2011) Removal of dyes from wastewaters by adsorption on pillared clays, ***Chemical Engineering Journal***, **168:** 1032-1040.
17. V. K. Garg, M. Amita, R. Kumar, R. Gupta, (2004) Basic dye (methylene blue) removal from simulated wastewater by adsorption using Indian Rosewood sawdust: A timber industry waste, ***Dyes and Pigments***, **63:** 243-250.
18. S. Khalili, B. Khoshandam, M. Jahanshahi, (2016) Synthesis of activated carbon/polyaniline nanocomposites for enhanced CO_2 adsorption, ***RSC Advances***, **6:** 35692-35704.
19. M. A. Khan, R. Govindasamy, A. Ahmad, M. R. Siddiqui, S. A. Alshareef, A. A. H. Hakami, M. Rafatullah, (2021) Carbon based polymeric nanocomposites for dye adsorption: Synthesis, characterization, and application, ***Polymers* (*Basel*)**, **13:** 419.
20. H. Ali, A. M. Ismail, (2023) Fabrication of magnetic Fe_3O_4/polypyrrole/carbon black nanocomposite for effective uptake of congo red and methylene blue dye: Adsorption investigation and mechanism, ***Journal of Polymers and the Environment***, **31:** 976-998.
21. N. B. Allou, A. Yadav, M. Pal, R. L. Goswamee, (2018) Biocompatible nanocomposite of carboxymethyl cellulose and functionalized carbon-norfloxacin intercalated layered double hydroxides, ***Carbohydrate Polymer***, **186:** 282-289.
22. N. Mabungela, N. D. Shooto, F. Mtunzi, E. B. Naidoo, M. Mlambo, K. E. Mokubung, S. Mpelane, (2023) Multi-application of fennel (Foeniculum vulgaris) seed composites for the adsorption and photo-degradation of methylene blue in water, ***South African Journal of Chemical Engineering***, **44:** 283-296.
23. C. S. Nkutha, N. D. Shooto, E. B. Naidoo, (2020) Adsorption studies of methylene blue and lead ions from aqueous solution by using mesoporous coral limestones, ***South African Journal of Chemical Engineering***, **34:** 151-157.
24. M. M. Felista, W. C. Wanyonyi, G. Ongera, (2020) Adsorption of anionic dye (Reactive black 5) using macadamia seed Husks: Kinetics and equilibrium studies, ***Scientific African***, **7**: e00283.
25. F. C. Wu, R. L. Tseng, R. S. Juang, (2009) Initial behavior of intraparticle diffusion model used in the description of adsorption kinetics, ***Chemical Engineering Journal***, **153:** 1-8.
26. O. A. Aworanti, S. E. Agarry, (2017) Kinetics, isothermal and thermodynamic modelling studies of hexavalent chromium ions adsorption from simulated wastewater onto parkia biglobosa-sawdust derived acid-steam activated carbon, ***Applied Journal of Environmental Engineering Science***, **3:** 58-76.
27. Saruchi, V. Kumar, (2019) Adsorption kinetics and isotherms for the removal of Rhodamine B dye and Pb^{+2} ions from aqueous solutions by a hybrid ion-exchanger, ***Arabian Journal of Chemistry***, **12:** 316-329.
28. A. A. Inyinbor, D. T. Bankole, F. A. Adekola, O. S. Bello, T. Oreofe, K. Amone, A. F. Lukman, (2023) Chemometrics validation of adsorption process economy: Case study of acetaminophen removal onto quail eggshell adsorbents, ***Scientific African***, **19**: e01471.
29. N. B. Allou, J. Saikia, R. L. Goswamee, (2018) Use of calcined Mg-Al layered double hydroxides to regulate endocrine disruptor methylparaben in excess as adsorbent and as control releasing agent in normal situations, ***Journal of Environmental Chemical Engineering***, **6:** 1189-1200.
30. L. A. Munoz, F. Pedreschi, A. Leiva, J. M. Aguilera, (2015) Loss of birefringence and swelling behavior in native starch granules: Microstructural and thermal properties, ***Journal of Food Engineering***, **152:** 65-71.
31. K. Dome, E. Podgorbunskikh, A. Bychkov, O. Lomovsky, (2020) Changes in the crystallinity degree of starch having different types of crystal structure after mechanical pretreatment, ***Polymers* (*Basel*)**, **12:** 641.
32. N. Sivarajasekar, R. Baskar, V. Balakrishnan, (2009) Biosorption of an AZO dye from aqueous solutions onto *Spirogyra*, ***Journal of the University of Chemical Technology and Metallurgy***, **44:** 157-164.
33. S. Yadav, A. Asthana, R. Chakraborty, B. Jain, A. K. Singh, S. A. C. Carabineiro, M. A. B. H. Susan, (2020) Cationic dye removal using novel magnetic/activated charcoal/β-cyclodextrin/alginate polymer nanocomposite, ***Nanomaterials* (*Basel*)**, **10:** 170.
34. E. Nyankson, J. Adjasoo, J. K. Efavi, A. Yaya, G. Manu, A. Kingsford, R. Y. Abrokwah, (2020) Synthesis and kinetic adsorption characteristics of Zeolite/CeO_2 nanocomposite, ***Scientific African***, **7**: e00257.
35. R. L. Tseng, S. K. Tseng, F. C. Wu, (2006) Preparation of high surface area carbons from corncob with KOH etching plus CO_2 gasification for the adsorption of dyes and phenols from water, ***Colloids and Surfaces A: Physicochemical and Engineering Aspects***, **279:** 69-78.
36. F. C. Wu, R. L. Tseng, (2008) High adsorption capacity NaOH-activated carbon for dye removal from aqueous solution, ***Journal***

of Hazardous Materials, **152:** 1256-1267.
37. A. Salisua, M. M. Sanagi, A. A. Naim, K. J. Karim, (2015) Removal of methylene blue dye from aqueous solution using alginate grafted polyacrylonitrile beads, ***Der Pharma Chemica***, **7:** 237-242.
38. J. S. Piccin, G. L. Dotto, L. A. A. Pinto, (2011) Adsorption isotherms and thermochemical data of FD&C Red N° 40 binding by chitosan, ***Brazilian Journal of Chemical Engineering***, **28:** 295-304.
39. T. K. Saha, S. Karmaker, H. Ichikawa, Y. Fukumori, (2005) Mechanisms and kinetics of trisodium 2-hydroxy-1,1'-azonaphthalene-3,4',6-trisulfonate adsorption onto chitosan, ***Journal of Colloid and Interface Science***, **286:** 433-439.
40. K. S. Baidya, U. Kumar, (2021) Adsorption of brilliant green dye from aqueous solution onto chemically modified areca nut husk, ***South African Journal of Chemical Engineering***, **35:** 33-43.

****Bibliographical Sketch***

Dr. N. B. Allou is currently working as Senior Assistant Professor in the laboratory of Material Constitution and reaction, University of Félix Houphouet Boigny, Cote d'Ivoire. He obtained his PhD degrees in Chemical Science in 2018 from Academy of Scientific and Innovative Research, India. He has more than 15 research publications to his credit, published international journals. His research is focused on development of bioadsorbant and hybrid nanocomposite drug delivery system.